Patterned nanostructure in AgCo/Pt/MgO(001) thin films

Zhi-Rong Liu and Huajian Gao
Max Planck Institute for Metals Research, Heisenbergstrasse 3, D-70569 Stuttgart, Germany

L. Q. Chen
Department of Materials Science and Engineering, The Pennsylvania State University, University Park, Pennsylvania 16802, USA

Kyeongjae Cho
Mechanics and Computation Division, Mechanical Engineering Department, Stanford University, Stanford, California 94305, USA
(Received 11 February 2003; published 30 July 2003)

The formation of a patterned nanostructure in an AgCo/Pt/MgO(001) thin film is simulated by a technique of combining molecular dynamics and phase-field theory. The dislocation (strain) network existing in Pt/MgO is used as a template whose pattern is transferred to the AgCo phase in spinodal decomposition, resulting in regular arrays of Co islands that are attracted by the dislocations. The influence of various factors, such as the component concentration and film thickness, is studied. It is found that the spinodal decomposition of AgCo in this system is mainly characterized by a competition between a surface-directed layer structure and the strain-induced patterned structure, where the patterned Ag-Co structure only dominates in a small range near the interface (less than ten atomic layers). However, if the interlayer diffusion can be minimized by controlling film growth conditions, it is shown that the patterned structure can be formed throughout the entire film.

DOI: 10.1103/PhysRevB.68.035429 PACS number(s): 68.55.−a, 64.75.+g, 81.16.Rf, 81.30.Hd

I. INTRODUCTION

With the rapid development of the high-density information storage device, the control of grain size and grain size distribution in magnetic thin films will be required for the next generation of information storage technology, where the drive for decreased media noise and increased storage density is pushing the grain size below the 10-nm regime.[1,2] The present technology involves the deposition of Co rich magnetic phases onto seed layers whose grain size determines the grain size of the magnetic layer through grain to grain epitaxy. For example, in IBM's 10 Gbit/in.^{2} demonstration, a magnetic film with an average grain size of 12 nm is obtained, where a Co phase is deposited onto NiAl seed layers.[2] Other methods to control grain size and grain size distribution were also explored in the labs. It was shown recently that monodispersed magnetic nanoparticles can be created by chemical means and deposited onto a substrate to form a highly regular array of particles.[3]

There are several possibilities for introducing controllable lengthscales into the film formation process, one of which is the self-organized growth on a substrate with a preferred nanopattern. For example, flat nanosized Co dots form in a Au(111) substrate with surface reconstruction,[4] and ordered arrays of vertical magnetic Co pillars can be further obtained by alternative deposition of Co and Au layers.[5] When a Co film is deposited on the Pt(111), fcc and hcp phases are arranged in regular patterns to reduce the strain energy.[6] Recently, Kern *et al.* showed that the strain-relief dislocation network in a substrate can be transferred through heterogeneous nucleation to a regular superlattice of almost monodispersed islands with great feasibility.[7]

In a previous paper,[8] the interaction between the spinodal decomposition of thin film and the dislocation network of substrate was briefly discussed, with an AgCo/Pt/MgO thin film as an example. It was revealed that Co phases are attracted by dislocations in the Pt/MgO interface, producing an interesting nanostructure. Such a mechanism may provide the possibility to control the length scale for a magnetic recording media layer. For example, after the patterned nanostructure of AgCo phases is established in spinodal decomposition as a seed layer, a Co-rich conventional medial alloy can grow on it. In this paper, detailed simulations are conducted in an AgCo/Pt/MgO(001) thin film to investigate the formation of a nanostructure under various conditions.

II. THEORETICAL MODEL AND SIMULATION METHOD

A. System model

The system considered here is the AgCo/Pt/MgO(001) thin film (see Fig. 1). MgO is the preferred substrate material in many of the new information storage and processing devices made from thin metal films.[9] MgO has a fcc lattice structure with lattice parameter $a_{\mathrm{MgO}}=4.21$ Å, which is slightly larger than that of Pt ($a_{\mathrm{Pt}}=3.924$ Å). When a Pt film

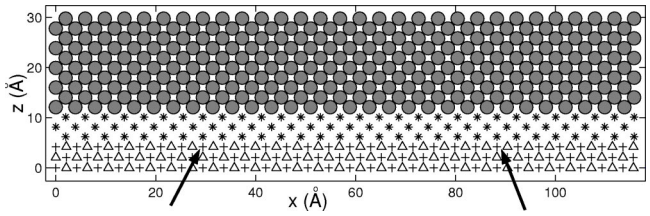

FIG. 1. Schematic graphics of the AgCo/Pt/MgO(001) thin film. The symbols cross (+), triangle (△), and stars (*) represent atoms Mg, O, and Pt, respectively, while the filled circle (●) for AgCo atoms. Pt atoms trend to sit atop the surface O atoms due to their favorable interaction energy. The arrows indicate the locations where dislocation will be generated. Axes are plotted in units of Å.

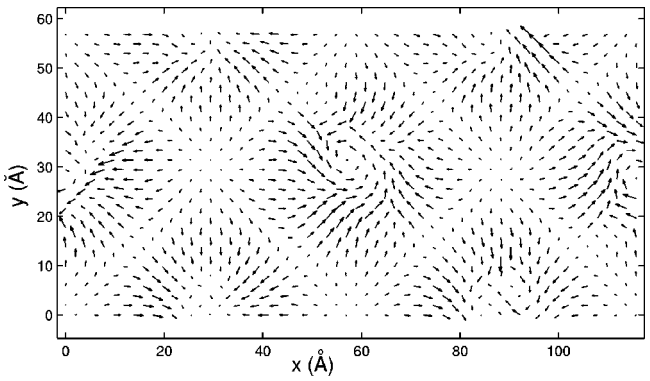

FIG. 2. The strain effect of the as-grown Pt/MgO(001) thin film that is represented by nonuniform atomic displacements on the surface. A system with 3 ML of Pt is simulated, and the displacements of surface atoms are plotted.

is deposited on a MgO substrate, due to the interactions between the film and substrate the Pt phase will be subject to elastic mismatch strain. The mismatch strain energy is partly released by the formation of an interfacial dislocation network.[10] The dislocation network of Pt/MgO(001) with a cube-on-cube orientation relationship appears as a square net with a dislocation spacing of 4.05 nm. Such a dislocation network results in periodic variations of the strain in Pt thin film (see Fig. 2). It has been pointed out by theoretical analysis[11] and simulation[8] that such periodic strain provides a nanopattern for the spinodal of a second film on it. In this paper, we consider an AgCo thin film on the strained Pt/MgO(001) (Fig. 1), and simulate the spinodal decomposition of the AgCo phase. As in most simulations on spinodal decomposition, the atoms of the initial AgCo phase are randomly arranged in a regular (fcc) crystal lattice. The model assumes that AgCo is deposited on Pt/MgO in a disordered state, and we calculate the formation of nanostructure by a subsequent annealing process.

B. Simulation method

There are a number of approaches proposed to model the elastic effect on precipitate morphology in coherent systems,[12] where the linear elasticity theory is employed to calculate the elastic energy. In this paper, we adopt an alternative method[8,13] of combining atomistic calculations and microscopic mean-field theory, which is applicable for noncoherent cases, to simulate the effect of dislocation, strain response, and spinodal decomposition in an AgCo/Pt/MgO(001) thin film. In this study, the morphology of the system is described by the position and occupation probability (atomic concentration) of all atoms, $\{\mathbf{r}_i, n_i\}$. $\{\mathbf{r}_i\}$ are used to simulate local atomic motion such as strain response or dislocation, while $\{n_i\}$ are used to simulate atomic diffusion of phase transformation. The atomic concentrations of MgO and Pt phases are fixed in simulation, while the AgCo phase undergoes a process of spinodal decomposition. After expressing the empirical potential and free energy as functions of $\{\mathbf{r}_i, n_i\}$ under a mean-field approximation, i.e., $V(\{\mathbf{r}_i, n_i\})$ and $F(\{\mathbf{r}_i, n_i\})$, the evolution of atomic positions is given in molecular dynamics (MD) as[14]

$$m_i \frac{d^2\mathbf{r}_i}{dt^2} = -\nabla_i V(\{\mathbf{r}_i, n_i\}), \tag{1}$$

while the diffusion process is described in microscopic mean-field theory as[15,16]

$$\frac{dn_i}{dt} = \sum_j L_{ij} \frac{\partial F(\{\mathbf{r}_i, n_i\})}{\partial n_j}, \tag{2}$$

where L_{ij} is the kinetic coefficient proportional to the inverse average time of elementary diffusional jumps from site i to j. The time scale of diffusion is mainly determined by the magnitude of L_{ij}. In our calculation, L_{ij} is assigned as a constant L when $|\mathbf{r}_i - \mathbf{r}_j| < R_{\text{diff}}$, and 0 otherwise. Since diffusion is much slower than the elastic response, the system is set in elastic equilibrium during the diffusion process. In a numerical scheme, the simulation loop is as follows: (1) run m steps of MD by Eq. (1) with a time step δt to reach elastic equilibrium; (2) run one step of diffusion by Eq. (2) with a time step dt; and (3) go to (1). It is a multiscale scheme overcoming the weakness of small time scale in MD, since $m\delta t \ll dt$. Although the present work employed a microscopic diffusion equation for a binary system and assumed an atomic exchange mechanism for diffusion, it is rather straightforward to formulate the microscopic diffusion using a vacancy mechanism by introducing the vacancy as the third component. With the vacancy as the third component, the model can automatically model the surface morphology changes as a result of surface energy anisotropy and the balance of surface energies and the interphase boundary energy between the two phases in the film.[17] However, as a first attempt, we assumed a simple exchange mechanism. The vacancy mechanism will be considered in a future publication.

C. Empirical potential

The empirical potential between Ag, Co, and Pt atoms adopted in the current simulation is the tight-binding second-moment-approximation (TB-SMA) scheme,[18] where the potential is comprised of a binding part and a repulsive part:

$$V = \sum_i (E_R^i + E_B^i). \tag{3}$$

For the AgCo phase, to include the influence of atomic concentration, the following formula is used under mean-field approximation for the potential (A and B denote two atomic species, Ag and Co, respectively, and n_i, and n_j are the concentrations of A atoms):

TABLE I. TB-SMA parameters for Ag-Co-Pt.

	A (eV)	ξ (eV)	p	q	r_0 (Å)
Ag-Co	0.0752	1.1944	11.261	2.7127	2.696
Ag-Pt	0.1988	1.9399	10.770	3.5711	2.832
Co-Pt	0.1449	1.9959	11.108	3.145	2.667

$$E_R^i = \sum_j \left\{ \begin{array}{l} n_i n_j A_{\mathrm{AA}} \exp[-p_{\mathrm{AA}}(r_{ij}/r_0^{\mathrm{AA}}-1)] \\ +[n_i(1-n_j)+(1-n_i)n_j]A_{\mathrm{AB}}\exp[-p_{\mathrm{AB}}(r_{ij}/r_0^{\mathrm{AB}}-1)] \\ +(1-n_i)(1-n_j)A_{\mathrm{BB}}\exp[-p_{\mathrm{BB}}(r_{ij}/r_0^{\mathrm{BB}}-1)] \end{array} \right\}, \tag{4}$$

$$E_B^i = -\left\{ \sum_j \left[\begin{array}{l} n_i n_j \xi_{\mathrm{AA}} \exp[-q_{\mathrm{AA}}(r_{ij}/r_0^{\mathrm{AA}}-1)] \\ +[n_i(1-n_j)+(1-n_i)n_j]\xi_{\mathrm{AB}}\exp[-q_{\mathrm{AB}}(r_{ij}/r_0^{\mathrm{AB}}-1)] \\ +(1-n_i)(1-n_j)\xi_{\mathrm{BB}}\exp[-q_{\mathrm{BB}}(r_{ij}/r_0^{\mathrm{BB}}-1)] \end{array} \right]^2 \right\}^{1/2}, \tag{5}$$

where r_{ij} represents the distance between atoms i and j and $r_0^{\alpha\beta}$ is the first-neighbor distance in the $\alpha\beta$ lattice. A, p, ξ, and q are some free parameters of the SMA scheme that are fitted to desired properties of the system. The parameters for the pure species are available in the literature.[18] For the cross parameters of Ag-Co interaction, we fit A, ξ to the heat of formation (+26 kJ/g atom) (Ref. 19) and the lattice parameter (3.81 Å that is assumed to be the average value between pure Ag and Co) of the $Ag_{0.5}Co_{0.5}$ disordered phase, while p and q are simply assigned to the average values of pure species. The result obtained is shown in Table I. Based on the potential scheme Eqs. (3)–(5) and the fitted parameters, the formation heat and the lattice constant at any atomic concentration can be calculated, which are depicted as Fig. 3. The curve of the formation heat can be described by the parabolic law very well. Approximately, the lattice constant of the disordered alloy varies linearly with the atomic concentration, which is known as Vegard's law.[20] The elastic constants are also calculated (see Fig. 4). It appears that the elastic constants monotonically change with the concentration. However, it should be noted that the curves do not satisfy the linear law that is assumed by many spinodal decomposition simulations.

The cross parameters of Ag-Pt and Co-Pt are also listed in Table I, which are fitted in a similar process. The heat of formation is assumed to be zero for the lack of experimental data. The heat of formation will affect the behaviors of atomic diffusion. However, the atomic concentrations of Pt phase are fixed in our model, and no diffusion is considered between the Pt and Ag phases or Pt and Co phases. So the exact value of the heat of formation is not important for the process investigated in this paper.

The importance of the Pt/MgO substrate in the current simulation lies in its dislocation network and the corresponding strain effect. We keep the MgO atoms fixed in simulation and describe the interactions between Pt and MgO as the Lenard-Jones potential:

$$V_{\mathrm{LJ}} = 4\varepsilon\left[\left(\frac{\sigma}{r}\right)^{12} - \left(\frac{\sigma}{r}\right)^{6}\right]. \tag{6}$$

The parameters are adopted as $\varepsilon_{\text{Mg-Pt}} = 0.336$ eV, $\sigma_{\text{Mg-Pt}} = 2.3$ Å, $\varepsilon_{\text{O-Pt}} = 1.34$ eV, and $\sigma_{\text{O-Pt}} = 1.783$ Å, with a distance cutoff 3.4 Å. With these parameters, isolated Pt atoms can be adsorbed by MgO substrate by sitting 1.99 Å atop the surface O atoms of MgO(001) with an adsorption energy of 2.35 eV as indicated by density-functional calculations.[21] A MD simulation shows that such a potential can produce dislocation network as required and the corresponding periodic strain (see Fig. 2).

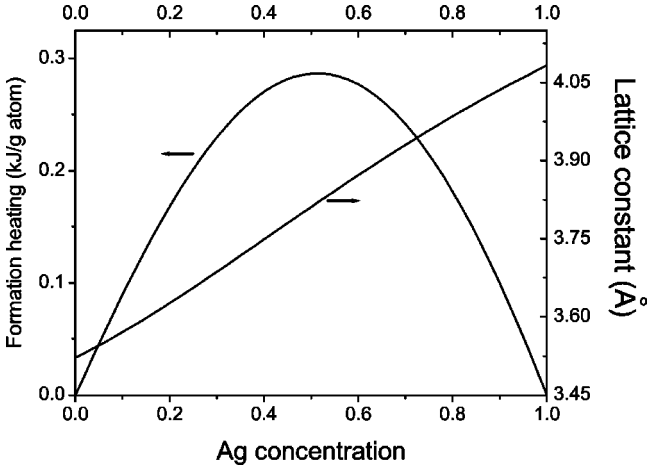

FIG. 3. Heat of formation and lattice constant of the disordered AgCo phase as functions of Ag concentration. The curves are calculated by using the mean-field TB-SMA potential [Eqs. (3)–(5)] with parameters in Table I.

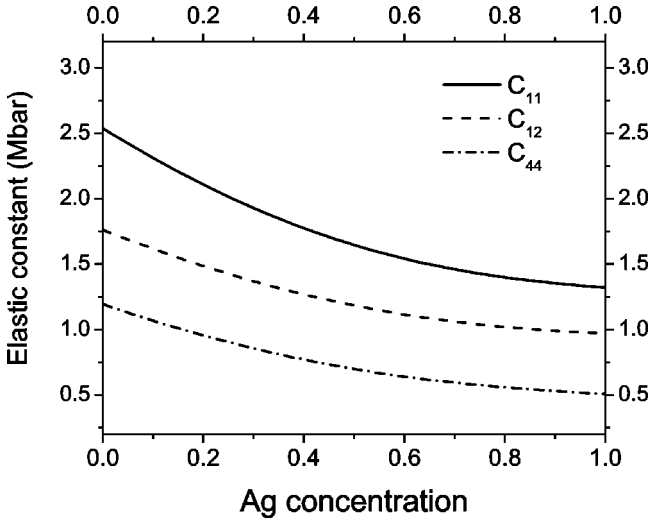

FIG. 4. Elastic constants of disordered AgCo phase as functions of Ag concentration under the mean-field TB-SMA potential.

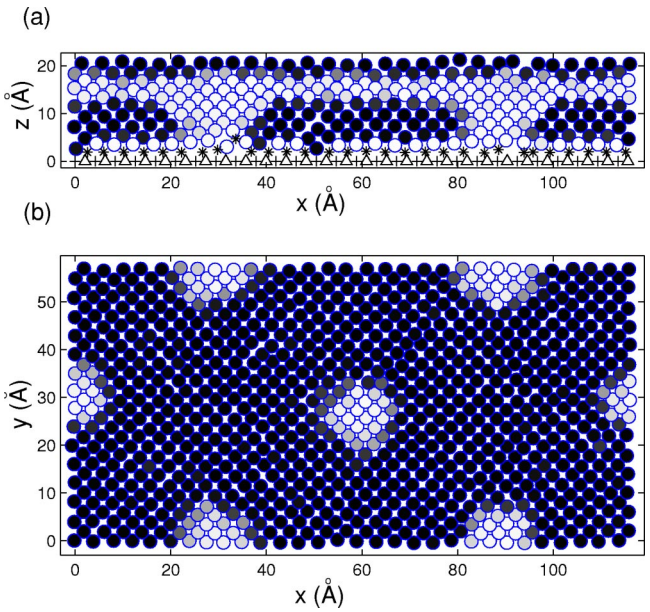

FIG. 5. Atomic configuration of the system with 1 ML of Pt and 10 ML of AgCo ($c_{Ag}=0.5$) at $t^*=70$. 240000 molecular dynamics steps are used. The symbols +, △ and * represent Mg, O, and Pt atoms, respectively. The occupation probability n_i of AgCo atoms is visualized by the filling darkness of the circle at $\mathbf{r}_i$, with white representing low value (Co) and black representing high value (Ag). (a) The x-z monolayer located at $y=0$. (b) The third x-y monolayer of the AgCo phase (counting from the bottom to the surface).

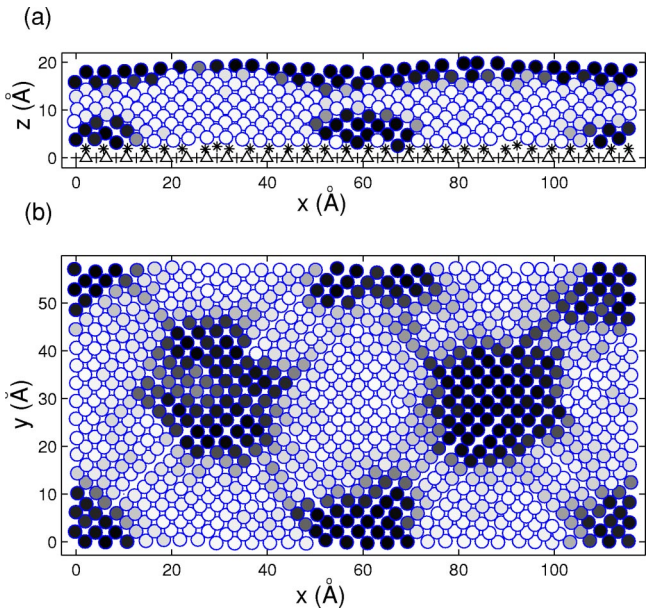

FIG. 6. Snap-shot of phase morphologies of the system with 1 ML of Pt and 10 ML of AgCo ($c_{Ag}=0.25$). (a) The x-z monolayer located at $y=0$. (b) The second x-y monolayer of the AgCo phase.

III. RESULTS AND DISCUSSIONS

A. Basic feature

A three-dimensional (3D) system of an AgCo/Pt/MgO(001) thin film with 1 ML of Pt and 10 ML of AgCo phase is simulated. Every monolayer (in the xy plane) contains 30×30 AgCo atoms, and periodic boundary conditions are applied in x and y axes. A free boundary condition is used in the z axis. The average Ag concentration is $c_{Ag}=0.5$. The diffusion cutoff in one diffusion step is $R_{diff}=3.53$ Å, i.e., $L_{ij}=L$ for the nearest neighbors and $L_{ij}=0$ in other cases. A reduced time is defined as $t^*=t/L$ to measure the simulation process. The time step of the MD is kept as $\delta t=0.15\times10^{-15}$ s, and the temperature is 600 K. The time step of the diffusion simulation is dynamically adjusted to ensure the convergence of the result.

The simulation result corresponding to $t^*=70$ is depicted in Fig. 5. 240000 MD steps are conducted in the simulation. We can see that the surface of thin film is covered by Ag phase. The reason is that the surface energy of Ag (1.3 J/m^2) is half that of Co (2.71 J/m^2).[22] A similar case occurs in the CuCo system, where the Cu phase will diffuse onto the surface to form a metastable alloy in epitaxial growth.[23] Due to the influence of the surface, AgCo is decomposed into a layer structure near the surface. In fact, it is a kind of surface-directed spinodal decomposition.[24] An interesting phenomenon is observed near the AgCo/Pt interface: Co atoms are attracted to the strained regions near the dislocations because their atomic radii are smaller than that of Ag. As a result, the AgCo decomposed phase produces an interesting 2D nanostructure pattern [Fig. 5(b)]. So the basic feature of spinodal decomposition in an AgCo/Pt/MgO(001) system can be described as a competition between the surface-directed layer structure and the substrate-dislocation-induced nanopattern. These features are consistent with previous results in the 2D approximation.[8]

B. Effect of AgCo concentration

In this section, we investigate the effect of the AgCo concentration on the spinodal decomposition. Two Ag concentrations, $c_{Ag}=0.25$ and 0.75, are considered, and the results are compared with that of $c_{Ag}=0.5$ in Sec. III A.

A result of $c_{Ag}=0.25$ is given in Fig. 6. The layer structure near the surface is similar to the case of $c_{Ag}=0.5$. The difference occurs in the nanostructure near the interface: due to the reduction of the Ag concentration, Ag-rich regions near the interface shrink in volume, and the nanopattern changes from Co islands in the Ag matrix [Fig. 5(b)] into Ag islands in the Co matrix [Fig. 6(b)]. When the system evolves in a longer time, it is observed in the simulation that the flat Ag islands get smaller and smaller. This means the surface Ag phase tends to absorb the Ag islands near the interface.

Now, we come to the case of $c_{Ag}=0.75$ (Fig. 7). Compared with the result of $c_{Ag}=0.5$, there is no layer structure of the Co phase near the surface in present case. All Co atoms condense as conelike islands on the dislocations of the substrate. They are covered by an Ag-rich phase that spread to the surface. When $c_{Ag}=0.5$, the Co phases near the interface also assume the shape of conelike islands [Fig. 5(a)], but the cones stand upside down, merging with the layer structure near the surface.

It is noted that the Ag phase is important in forming the Co islands in the above process. If there is no Ag phase, a Co

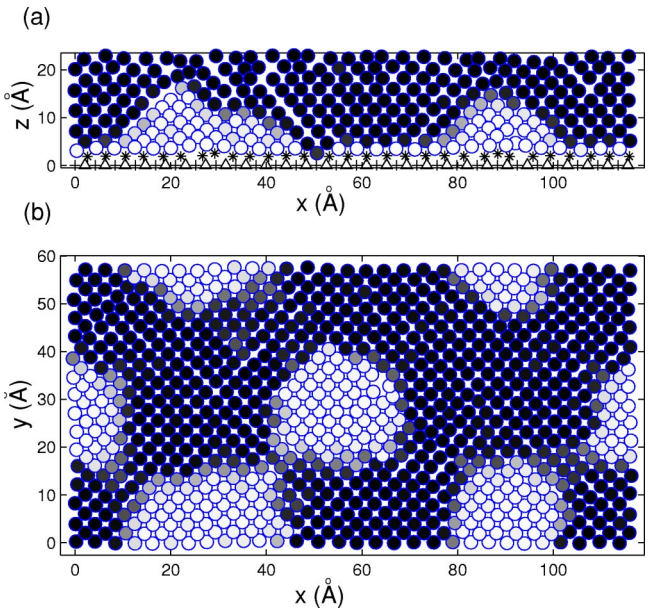

FIG. 7. Atomic configuration of the system with 1 ML of Pt and 10 ML of AgCo ($c_{\mathrm{Ag}}=0.75$). (a) The x-z monolayer located at $y=0$. (b) The third x-y monolayer of the AgCo phase.

thin film will grow in a layer structure at a small thickness. The Ag phase acts as an equivalent surfactant in assisting Co to decompose into islands. The present study suggests that it may be possible to produce a nanostructure by the following process. First, Co islands can be formed via spinodal decomposition of AgCo on a periodic strained substrate. Subsequently, the Ag phase can be removed by chemical etching, leaving a regular array of Co islands. Experiments will be needed to test this conjecture.

C. Effect of AgCo phase thickness

To explore the effect of the AgCo phase thickness, a system with 30 ML of AgCo with $c_{\mathrm{Ag}}=0.5$ is simulated with the result in Fig. 8. The basic characteristics are similar to the above results: a competition between the layer structure near the surface and the patterned structure near the interface. The patterned structure induced by the dislocations of the substrate decays within a distance of about ten monolayers while the layer structure presides in most regions. The surface energy is of the same order as the atomic cohesive energy while the strain energy is a higher order variation of the cohesive energy. So the surface effect dominates at the current film thickness.

In order to quantitatively analyze the competition between two kinds of structures, we define the pattern correlation function of two layers as

$$R_{mn}=\frac{\mathbf{V}_m\cdot\mathbf{V}_n}{|\mathbf{V}_m|\cdot|\mathbf{V}_n|}-R^0_{mn}, \tag{7}$$

where $\mathbf{V}_m$, $\mathbf{V}_n$ are vectors composed of atomic concentrations within layers m and n. R^0_{mn} is the calculation result when there is no correlation between two patterns:

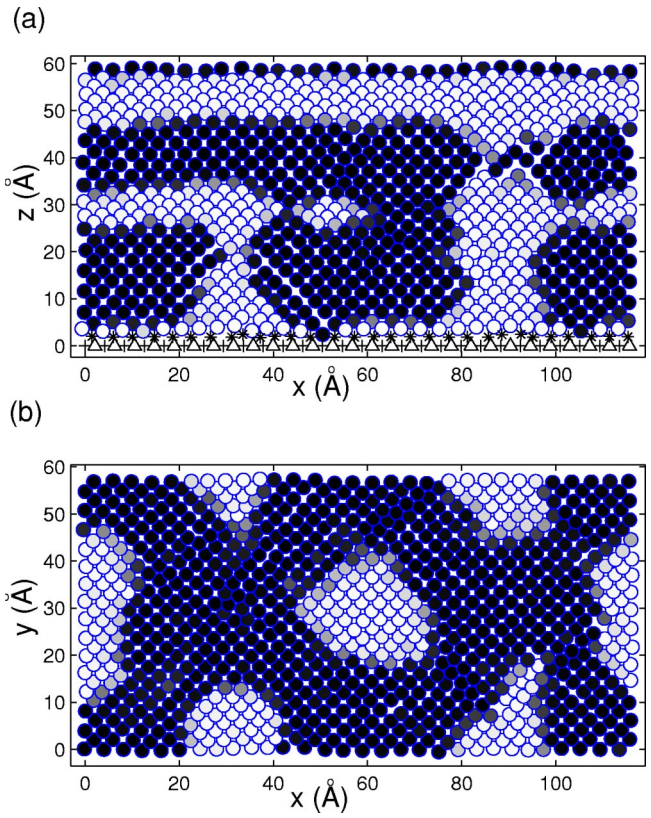

FIG. 8. Atomic configuration of the system with 1 ML of Pt and 30 ML of AgCo ($c_{\mathrm{Ag}}=0.5$). (a) The x-z monolayer located at $y=0$. (b) The third x-y monolayer of the AgCo phase.

$$R^0_{mn}=\frac{\sum_\mu V_{m\mu}\cdot\sum_\nu V_{n\nu}}{N_{\mathrm{layer}}|\mathbf{V}_m|\cdot|\mathbf{V}_n|}, \tag{8}$$

where $V_{m\mu}$ are components of $\mathbf{V}_m$ and N_{layer} is the number of components.

The third AgCo layer has a representative pattern induced by the dislocation of the substrate. We calculate the correction function of all AgCo layers with respect to the third one, and plot the result in Fig. 9, together with the layer concentration. It is clearly demonstrated that surface-directed spinodal decomposition (dashed line) penetrates throughout the thin film while the pattern structure (solid line) only exists in the range of ten monolayers near the interface. It suggests that the film thickness should be limited to small values if one is interested in producing a nanostructure by spinodal decomposition on a strained substrate. For example, when the thickness of AgCo phase decreases to 5 ML, a regular array of Co islands can be obtained in simulation (see Fig. 10).

D. Effect of Pt thickness

The strain induced by the dislocation declines in the Pt phase. If the thickness of the Pt phase is large, the strain acting on the AgCo phase will be too weak to induce a nanopattern.

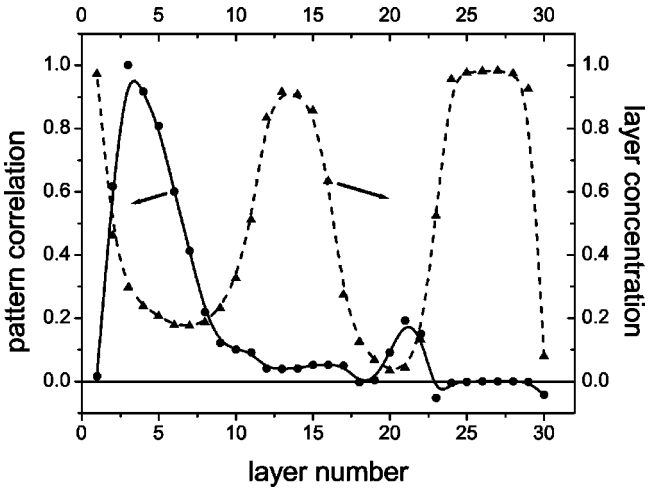

FIG. 9. Pattern correlation function (solid line and circles) and layer Ag concentration (dashed line and triangles) of AgCo phase in the system with 1 ML of Pt and 30 ML of AgCo ($c_{Ag}=0.5$). The pattern correlation function is normalized to make sure the self-correlation is equal to 1 ($R_{mm}=1$ for $m=3$ in this case).

Figure 11 displays the simulation results on the system with 3 ML of Pt and 30 ML of AgCo. It can be seen that there are only two Co islands within the simulation domain, in contrast to four islands in the previous cases. The other two Co islands, located at $y=30$ Å in the system with 1 ML of Pt, now disappear. This means that the strain spreading through 3 ML of Pt is losing its capability of attracting Co atoms to form islands. 3 ML is the critical thickness of Pt phase to produce patterned structure in the current case.

It has been illuminated in the previous sections that the influence of the surface competes with that of the dislocation strain. With a decreasing AgCo thickness, the structure near the interface is more and more affected by the surface. We conduct a simulation on the system with 3 ML of Pt and 10 ML of AgCo. Co islands appear only in the very early stage, and the final structure is a complete layer structure without any Co island.

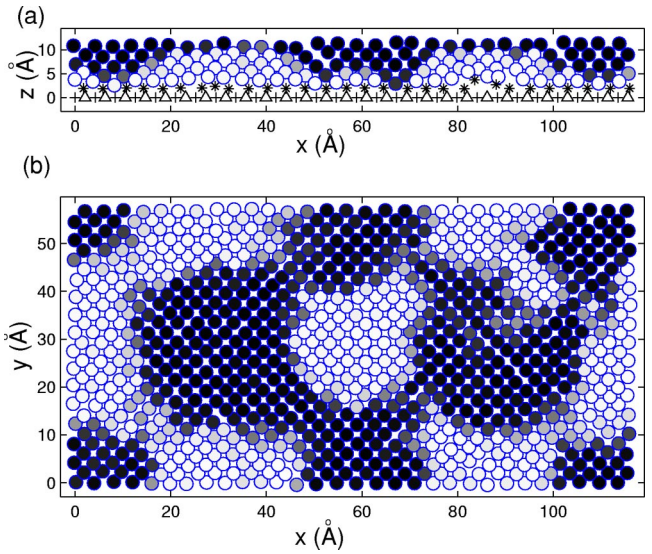

FIG. 10. Atomic configuration of the system with 1 ML of Pt and 5 ML of AgCo ($c_{Ag}=0.5$). (a) The x-z monolayer located at $y=0$. (b) The third x-y monolayer of the AgCo phase.

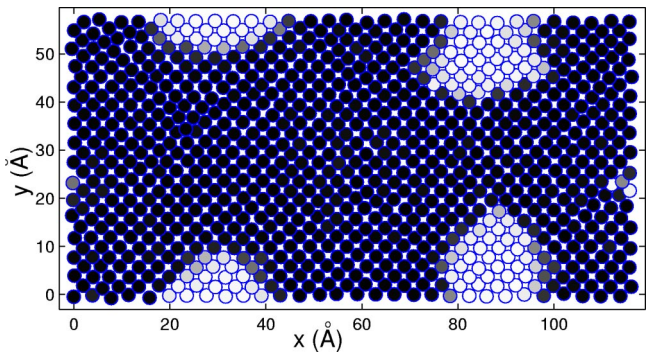

FIG. 11. Atomic configuration of the system with 3 ML of Pt and 30 ML of AgCo ($c_{Ag}=0.5$). The third x-y monolayer of the AgCo phase is depicted here.

Our analysis suggests there exists a critical value for the periodic strain of substrate to induce nanostructure in thin film. A previous study[11] indicated that the imposed strain provides a pre-existing preference wavelength for the spinodal decomposition in the initial stage, regardless of how small the strain is. The simulation results in this section shows that such a preference wavelength may be lost in the later stage, and that the self-organized nanostructure may fail to be realized if the strain is less than a critical value.

E. Film growth: layer by layer

The above research simulates the annealing process of the disordered AgCo phase where atomic diffusion occurs in the whole thin film (bulk diffusion). In experiments, surface diffusion is much faster than bulk diffusion. In the epitaxial growth of a thin film, the system is produced layer by layer. If one controls growth conditions carefully to prohibit interlayer diffusion while fully permitting intralayer diffusion, the resulting nanostructure can be markedly different (an interesting example in experiment is the formation of a metastable CuCo alloy in thin film[23]). We have simulated such a growth process by confining the diffusion to within each layer. The result of a system with 10 ML of AgCo and $c_{Ag}=0.75$ is plotted in Fig. 12. No layer structure is observed since interlayer diffusion is prohibited. The patterned nanostructure near the interface penetrates through the whole film to the surface. This would result in the phenomena of growth on seed layer, in which case an as-grown AgCo layer influenced by the substrate strain and shape in the nanopattern acts as a seed layer for the forthcoming growth. Since AgCo is a system with spinodal decomposition, an Ag atom is attracted to an Ag atom, and Co to Co, so that the nanopattern of the as-grown layer is transferred as the film grows.

Another possible way to suppress the surface-directed layer effect is to make use of the atmosphere of the film growth. In this paper, the film growth and spinodal decomposition are assumed to occur in a vacuum. Actually, the surface energies of the two metals will change in an atmosphere that is not a vacuum, and the relative magnitude could

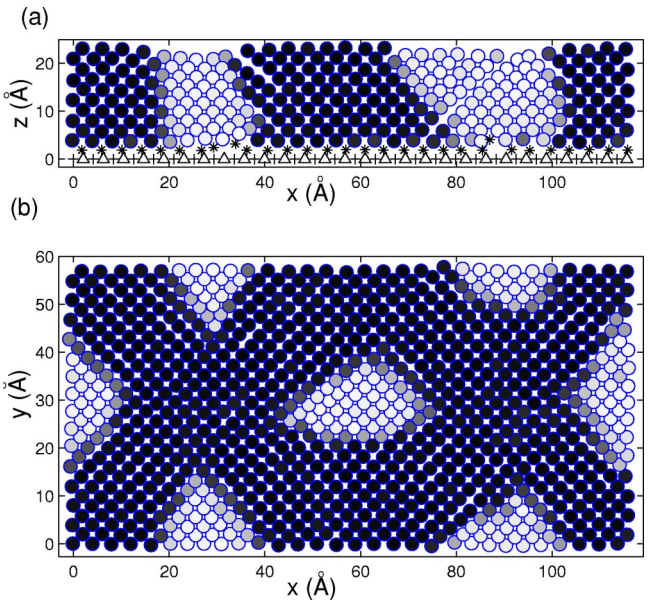

FIG. 12. Atomic configuration of the thin film grown layer by layer where atomic diffusion is restricted within the same layers. The system has 1 ML of Pt and 10 ML of AgCo ($c_{Ag}=0.75$). (a) The x-z monolayer located at $y=0$. (b) The third x-y monolayer of the AgCo phase.

in principle be reversed depending on the adsorbate. So the atmosphere has important influences on the final morphology. In particular, if the atmosphere is chosen to equalize the surface energies of the two metals, the surface-directed layer effect will disappear and a patterned nanostructure will be produced throughout the whole film. It is an interesting topic that is worthy of further investigating.

IV. CONCLUSIONS

Based on the above simulation results, it is concluded that a patterned nanostructure can be obtained in an AgCo/Pt/MgO thin film. The main feature of AgCo spinodal decomposition in this system is the competition between the surface-directed layer structure and the strain-induced patterned structure. The strain effect is weaker than the surface effect in the current cases. The patterned Ag-Co structure occurs only within a short range near the interface (no more than 10 ML), and the thickness of the Pt phase should be small enough to effectively transfer the strain of dislocation in the Pt/MgO interface to the AgCo phase to produce a nanostructure. However, if spinodal decomposition of the AgCo phase occurs within monolayers by careful film growth controlling, a surface-directed layer structure will be prohibited and the patterned structure will form in a wide range.

ACKNOWLEDGMENTS

This work was supported by a Max Planck Post-Doc Fellowship for Z.L. and by the U.S. National Science Foundation through Grant No. CMS-0085569. The code of MD simulation in this work comes from the program GONZO of Stanford Multiscale Simulation Laboratory. H.G. also acknowledges support by a Yangze lecture professorship of China.

[1] D.E. Laughlin, B. Lu, Y.N. Hsu, J. Zou, and D.N. Lambeth, IEEE Trans. Magn. **36**, 48 (2000).
[2] J. Li, M. Mirzamaani, X. Bian, M. Doerner, S. Duan, K. Tang, M. Toney, T. Arnoldussen, and M. Madison, J. Appl. Phys. **85**, 4286 (1999).
[3] S. Sun, C.B. Murray, D. Weller, L. Folks, and A. Moser, Science **287**, 1989 (2000).
[4] B. Voigtländer, G. Meyer, and N.M. Amer, Phys. Rev. B **44**, 10 354 (1991).
[5] O. Fruchart, M. Klaua, J. Barthel, and J. Kirschner, Phys. Rev. Lett. **83**, 2769 (1999).
[6] E. Lundgren, B. Stanka, M. Schmid, and P. Varga, Phys. Rev. B **62**, 2843 (2000).
[7] H. Brune, M. Giovannini, K. Bromann, and K. Kern, Nature (London) **394**, 451 (1998).
[8] Z.R. Liu, H. Gao, and L.Q. Chen, ArXiv: cond-mat/0209344 (unpublished).
[9] B.M. Lairson, M.R. Visokay, R. Sinclair, S. Hagstrom, and B.M. Clemens, Appl. Phys. Lett. **61**, 1390 (1992).
[10] P.C. Mcintyre, C.J. Maggiore, and M. Nastasi, Acta Mater. **45**, 869 (1997).
[11] P. A. Greaney, D. C. Chrzan, B. M. Clemens, and W. D. Nix (unpublished).
[12] S.Y. Hu and L.Q. Chen, Acta Mater. **49**, 1879 (2001), and references therein.
[13] R. Lesar, R. Najafabadi, and D.J. Srolovitz, Phys. Rev. Lett. **63**, 624 (1989).
[14] M. P. Allen and D. J. Tildesley, *Computer Simulation of Liquids* (Clarendon, Oxford, 1996).
[15] A.G. Khachaturyan, Fiz. Tverd. Tela (Leningrad) **9**, 2595 (1967) [Sov. Phys. Solid State **9**, 2040 (1968)].
[16] L.Q. Chen and A.G. Khachaturyan, Acta Metall. Mater. **39**, 2533 (1991).
[17] M. Plapp and J.F. Gouyet, Phys. Rev. Lett. **78**, 4970 (1997).
[18] F. Cleri and V. Rosato, Phys. Rev. B **48**, 22 (1993).
[19] A.R. Miedema, Philips Tech. Rev. **36**, 217 (1976).
[20] L. Vegard, Z. Phys. **5**, 17 (1921); M.F. Thorpe and E.J. Garboczi, Phys. Rev. B **42**, 8405 (1990).
[21] A. Bogicevic and D.R. Jennison, Surf. Sci. **437**, L741 (1999).
[22] L.Z. Mezey and J. Giber, Jpn. J. Appl. Phys. **21**, 1569 (1982).
[23] G.L. Zhou, M.H. Yang, and C.P. Flynn, Phys. Rev. Lett. **77**, 4580 (1996).
[24] G. Krausch, C.A. Dai, E.J. Kramer, and F.S. Bates, Phys. Rev. Lett. **71**, 3669 (1993).